

The Hall effect in Ni-doped p-CdSb in a strong magnetic field

This article has been downloaded from IOPscience. Please scroll down to see the full text article.

2008 Semicond. Sci. Technol. 23 125001

(<http://iopscience.iop.org/0268-1242/23/12/125001>)

View [the table of contents for this issue](#), or go to the [journal homepage](#) for more

Download details:

IP Address: 82.151.111.197

The article was downloaded on 28/02/2013 at 08:47

Please note that [terms and conditions apply](#).

The Hall effect in Ni-doped p-CdSb in a strong magnetic field

R Laiho¹, A V Lashkul^{1,2}, K G Lisunov^{1,2,3}, E Lähderanta²,
M A Shakhov^{1,4} and V S Zakhvalinskii^{1,5}

¹ Wihuri Physical Laboratory, University of Turku, FIN-20014 Turku, Finland

² Department of Physics and Mathematics, Lappeenranta University of Technology, FIN-53851 Lappeenranta, Finland

³ Institute of Applied Physics, Academiei Str 5, MD-2028 Kishinev, Moldova

⁴ A F Ioffe Physico-Technical Institute, 194021 St Petersburg, Russia

⁵ Department of Physics, Belgorod State University, RUS-308015 Belgorod, Russia

Received 2 July 2008

Published 29 September 2008

Online at stacks.iop.org/SST/23/125001

Abstract

The Hall effect in single crystals of the group II–V semiconductor p-CdSb doped with 2 at% of Ni is investigated between $T = 1.5$ and 300 K in pulsed magnetic fields up to $B = 25$ T. The Hall resistivity, ρ_H , exhibits a nonlinear dependence on B , which is strongly pronounced below ~ 10 K but is still observed even up to 300 K. The analysis of $\rho_H(B)$ gives evidence for the presence of a positive normal and a negative anomalous contribution, $\rho_N = R_0 B$ and ρ_A , respectively. The temperature dependence of the (normal) Hall coefficient R_0 is determined by the activation of holes into the valence band with a small contribution of the itinerant holes from the acceptor band at lowest T . The dependence of ρ_A on T is quite different within two temperature intervals, being weak between ~ 50 and 300 K and very strong below ~ 50 K, the latter resembling that of the resistivity, ρ . Analysis of ρ_A below ~ 77 K demonstrates that it scales approximately as ρ^n with $n = 1.6 \pm 0.1$ within four decades of ρ_A and more than two decades of ρ . The anomalous Hall effect in p-CdSb:Ni is attributable to the presence of magnetic Ni-rich nanoclusters, whose properties have previously been investigated by the analysis of the magnetization data.

(Some figures in this article are in colour only in the electronic version)

1. Introduction

Nowadays, diluted magnetic systems are extensively investigated due to their possible application in spintronics [1]. Crystalline semiconductors doped with transition-metal elements represent two important classes of such systems demonstrating a spin-dependent electron transport: (i) those having microscopically homogeneous magnetization due to the incorporation of magnetic ions in the lattice, and (ii) those possessing a strongly inhomogeneous distribution of magnetization connected to nanosize magnetic particles (clusters) [1].

Recently, the group II–V semiconductor cadmium antimonide doped with Ni (p-CdSb:Ni) has attracted attention due to its interesting magnetic properties [2]. At a high doping level of Ni, needle-like micrometer-size NiSb inclusions are known to be formed in CdSb [3]. On the other hand,

an array of nanosize Ni-rich $\text{Ni}_{1-x}\text{Sb}_x$ precipitates has been produced in p-CdSb:Ni by reduction of the doping level down to 2 at% of Ni [2], attributing the weakly doped compound to the group (ii) of diluted magnetic systems above. Macroscopic samples of $\text{Ni}_{1-x}\text{Sb}_x$ are ferromagnetic (FM) at $x \leq 7.5\%$ [4, 5]. As a result of the formation of $\text{Ni}_{1-x}\text{Sb}_x$ nanoclusters, with an FM ordering of the internal Ni spins, a high aspect ratio and preferential orientation of the major axes, the magnetization of p-CdSb:Ni has already saturated at 300 K in the magnetic field $B \sim 2$ T, demonstrating a large anisotropy of the saturation magnetization: $M_s = 11.6$, 14 and 30 (in units of 10^{-4} emu g^{-1}) along the axes [1 0 0], [0 1 0] and [0 0 1] respectively. Magnetic irreversibility and spin-freezing phenomena or deviation of the zero-field-cooled susceptibility, $\chi_{\text{ZFC}}(T)$, from the field-cooled susceptibility, $\chi_{\text{FC}}(T)$, connected to the frustrated ground state are already observed in p-CdSb:Ni below room temperature and attain

maximum near the cluster blocking temperature $T_b \sim 100$ K. The broad peak of $\chi_{ZFC}(T)$ around T_b reflecting transition from superparamagnetic (SP) to spin-frozen (blocked) behavior also implies a broad-size distribution of the $\text{Ni}_{1-x}\text{Sb}_x$ clusters [2]. In addition, one should mention the presence of a diamagnetic (DM) contribution (at all T between 5 and 300 K) and a paramagnetic (PM) contribution (below ~ 50 K) to the net magnetization of p-CdSb:Ni [2]. The former is typical of undoped CdSb [6], whereas the latter reflects that the overwhelming majority of Ni does not enter the $\text{Ni}_{1-x}\text{Sb}_x$ nanoclusters, forming smaller clusters and/or single ions in the lattice. Hence, the volume fraction of the $\text{Ni}_{1-x}\text{Sb}_x$ phase, $\eta' \sim 0.01\%$ being well below the percolation threshold, makes the clusters completely independent (isolated), excluding either direct or indirect (due to the low concentration of the holes) interaction of their magnetic moments [2].

The resistivity, ρ , of p-CdSb:Ni in a zero-magnetic field is anisotropic [7], as well as in undoped p-CdSb [6], and is governed above ~ 2.5 K by activation of holes from the acceptor levels to the valence band with the activation energy $E_A = 2.45, 2.50$ and 2.85 meV in the samples 1, 2 and 3 oriented along the axes $[100]$, $[010]$ and $[001]$, respectively [7]. In fields between $B = 10$ and 15 T, E_A acquires a weak dependence on B according to the law $E_A \approx \beta B^{1/3}$, where $\beta = 1.64, 1.53$ and 1.19 meV $\text{T}^{1/3}$ for samples 1, 2 and 3 respectively [8]. The anisotropic variable-range hopping conductivity observed below 2.5 K at $B = 0$ transforms into the nearest-neighbor hopping conductivity (with the onset at ~ 4.2 K) above $B \sim 4$ T, reflecting reduction of magnetic disorder when B is increased [8]. Analysis of the hopping conductivity in zero and weak ($B < 6$ T) fields has yielded values of the acceptor concentration, $N_A = 3.61, 3.37$ and $2.51 \times 10^{16} \text{ cm}^{-3}$ in samples 1, 2 and 3, respectively [7], which are typical of undoped and weakly doped CdSb [6] and have been confirmed by investigations of the hopping conductivity into fields up to 30 T [8].

This work completes our investigations into the magnetic and galvanomagnetic properties of p-CdSb:Ni, which started in [2] and continued in [7, 8], and is dedicated to the Hall effect. The presence of the magnetic nanoclusters suggests the existence of an anomalous contribution to the Hall resistivity, ρ_H , as has been established in various diluted magnetic semiconductors exhibiting superparamagnetism [9–11]. On the other hand, the low value of η' in our material does not favor neglecting the normal component of ρ_H . In such conditions the application of high magnetic fields is expected to yield valuable information on both contributions, normal and anomalous, to the Hall effect in CdSb:Ni.

2. Results and discussion

Single crystals of CdSb doped with 2 at% of Ni were grown by the modified Bridgman method [6]; one can find further preparation details in [2]. X-ray diffraction investigations do not reveal the presence of the second phase (which, however, has been established unambiguously in the magnetization measurements [2]—see section 1), the ingots of volume $\sim 1 \text{ cm}^3$ have been found to possess the same orthorhombic

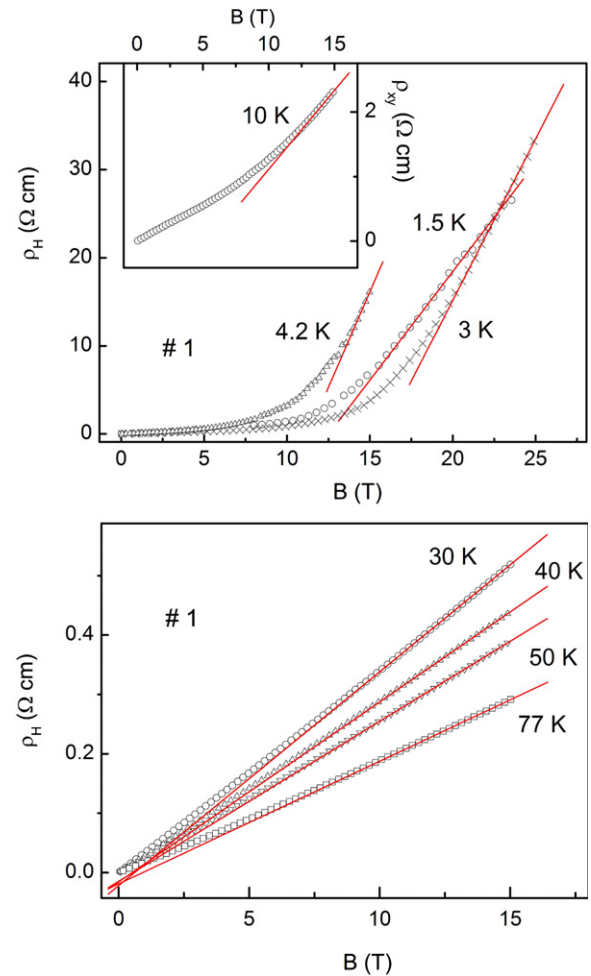


Figure 1. The plots of ρ_H versus B for sample 1. The lines are linear fits.

structure (space group D_{2h}^{15}) and lattice parameters as undoped CdSb. The growth direction of the ingots deviates by an angle of $50^\circ \pm 5^\circ$ from the $[100]$ axis. For investigations rectangular prisms of sizes $5.5 \times 1.9 \times 2.3 \text{ mm}^{-3}$, $5.5 \times 1.5 \times 2.3 \text{ mm}^{-3}$ and $5.5 \times 1.9 \times 2.0 \text{ mm}^{-3}$ with the longest edge along the $[100]$ (1), $[010]$ (2) and $[001]$ (3) axes, respectively, were cut from the ingots. The same samples have previously been used in the investigations into the longitudinal resistivity, ρ , and magnetoresistance [7, 8]. The measurements of ρ_H were made at constant temperatures between $T = 1.5$ and 300 K in pulsed magnetic fields up to $B = 25$ T in the transversal magnetic field configuration with $\mathbf{j} \parallel [100]$ and $\mathbf{B} \parallel [001]$ (1), $\mathbf{j} \parallel [010]$ and $\mathbf{B} \parallel [100]$ (2), $\mathbf{j} \parallel [001]$ and $\mathbf{B} \parallel [010]$ (3). The magnetic pulse length was 8 ms, the error in the strength of the field was not larger than 5% and its inhomogeneity did not exceed 0.3%.

The plots of ρ_H versus B are shown in figures 1–3 for samples 1, 2 and 3, respectively, exhibiting nonlinearity or strengthening of the dependence of $\rho_H(B)$ with increasing field, which is damped considerably when T is increased, being most pronounced below ~ 10 K but still persisting even up to 300 K. Another feature of the plots in figures 1–3, which is much less pronounced, is a weak inflection of ρ_H in the interval of $B < 10$ T at temperatures below ~ 10 K being

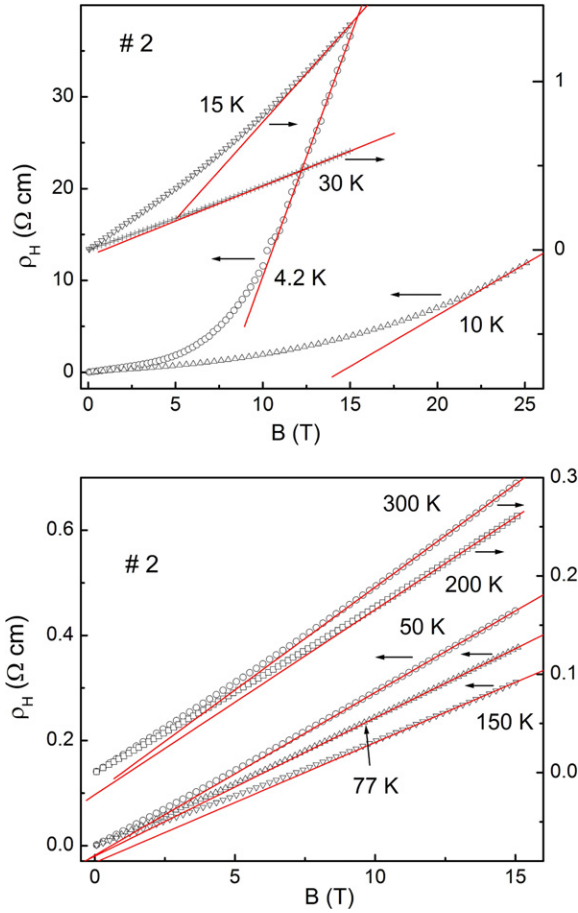


Figure 2. The plots of ρ_H versus B for sample 2. The lines are linear fits.

more observable for sample 1 (see the inset to the top panel of figure 1). Such a feature (clearly visible on the plots of R_H versus B , where $R_H \equiv \rho_H/B$) indicates the presence of two groups of the charge carriers (holes) typical of weakly doped or not intentionally doped p-CdSb [12], including those activated from acceptors to the valence band (VB) and occupying the extended (delocalized) states of the acceptor band (AB). In our case of p-CdSb:Ni contribution to the Hall effect from the itinerant holes of the AB is small, causing only a slight distortion of $\rho_H(B)$ in relatively weak fields, and at a reasonable approximation can be neglected (below we estimate this contribution more accurately).

In weakly doped non-magnetic semiconductors the nonlinearity of ρ_H or, equivalently, the magnetic-field dependence of R_H can appear due to the presence of the two groups of the charge carriers as mentioned above. However, for the same sign of the carriers (e.g. both groups are holes) this causes diminution of R_H with increasing B or the nonlinearity of ρ_H inverted with respect to that observed in figures 1–3, i.e., weakening of $\rho_H(B)$ when B is increased. The increase of $R_H(B)$ in strong fields can be connected to the presence of resonance bands and their complex behavior in a field, as has been observed, e.g., in n-CdSb [13]. However, in the weak-field interval such bands distort the dependences of $R_H(B)$ or $\rho_H(B)$ considerably, too [13], which does not take place in our case. Finally, the increase of the (normal) Hall

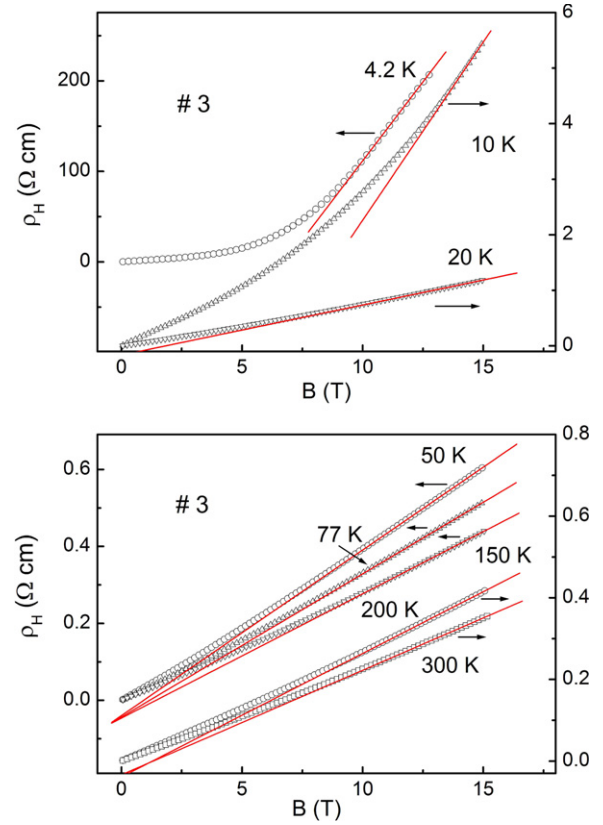


Figure 3. The plots of ρ_H versus B for sample 3. The lines are linear fits.

coefficient in high fields can be connected to magnetic freeze-out of the charge carriers or diminution of their concentration in the valence band, if the conductivity over the valence band is dominated, due to an increase of the activation energy in the magnetic field. However, it can be shown directly that this reason in our case is negligible due to a very weak dependence of $E_A(B)$ (see section 1).

Hence, the observed nonlinear behavior of $\rho_H(B)$ (neglecting a weak distortion in low fields) cannot be attributed to the reasons similar to those acting in non-magnetic doped semiconductors, but should be associated with the magnetic sub-system existing in p-CdSb:Ni (see section 1) due to an anomalous contribution to the Hall effect superimposed on the normal one.

In FM compounds the Hall resistivity is expressed by the equation

$$\rho_H = \rho_N + \rho_A, \quad (1)$$

where $\rho_N = R_0 B$ is the normal Hall resistivity, $\rho_A = R_s M$ is the anomalous contribution to ρ_H , M is the magnetization of the material, and R_0 and R_s are the normal (ordinary) and anomalous (spontaneous or extraordinary) Hall coefficients respectively [14, 15]. The coefficient R_0 governs the transversal electric field due to the Lorentz force acting on the charge carriers in the transversal magnetic field, and is determined presumably by their concentration (the classical Hall effect), whereas R_s is responsible for the generation of the transversal electric field of another nature, connected to the influence of the spin–orbit interaction on scattering of the spin-polarized electrons [14, 15].

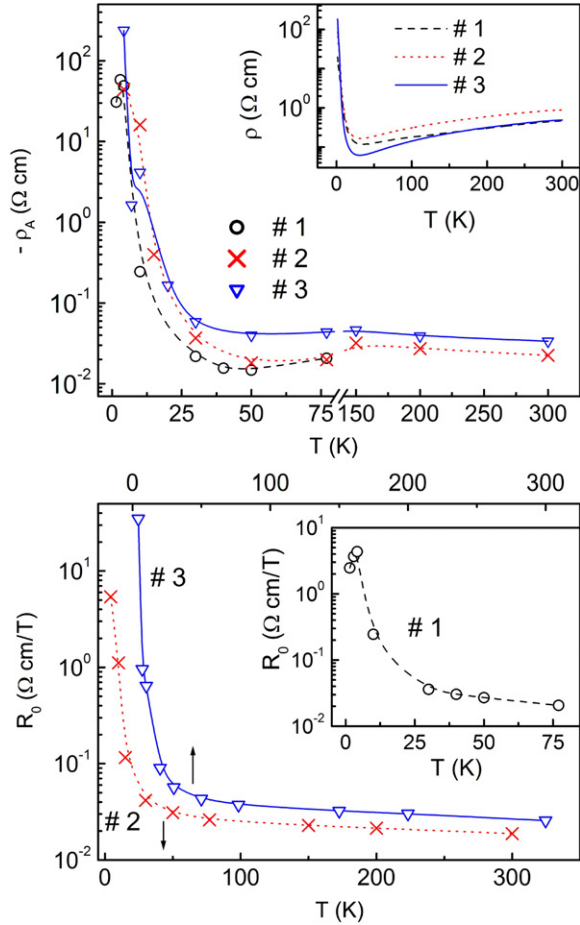


Figure 4. Temperature dependence of ρ_A (the top panel) and R_0 (the bottom panel) in the investigated samples. The lines are to guide the eye. Inset to the top panel: the plots of ρ versus T [7].

Generally, the anomalous Hall effect (AHE) is observed not only in purely FM compounds, and so the observation of this phenomenon cannot be regarded as a proof of an FM state [9]. At this point, the utilization of equation (1) for the interpretation of the Hall effect, which has been done (sometimes with modifications) in a variety of diluted magnetic semiconductors [9–11, 16, 17] or other types of magnetic materials, as, e.g., the colossal magnetoresistive oxides [17–19], should be performed with a certain caution, regarding it only as a phenomenological equation with limited applicability. Such applicability in our case of evidently non-FM compound can partially be substantiated by saturation of the magnetization when B is increased taking place already at 300 K (see section 1), so that the second term in equation (1) becomes independent of B and the plots of ρ_H versus B should tend to linear functions. Indeed, as follows from figures 1–3, such a tendency takes place in strong magnetic fields, permitting us to determine R_0 and ρ_A in a standard way, as the angular coefficient and the interception point with the ρ_H axis, respectively. The dependences of R_0 and ρ_A on T are shown in figure 4.

As can be seen from the bottom panel of figure 4, R_0 is positive (which can be expected for a p-type semiconductor with dominated conductivity over extended states) and

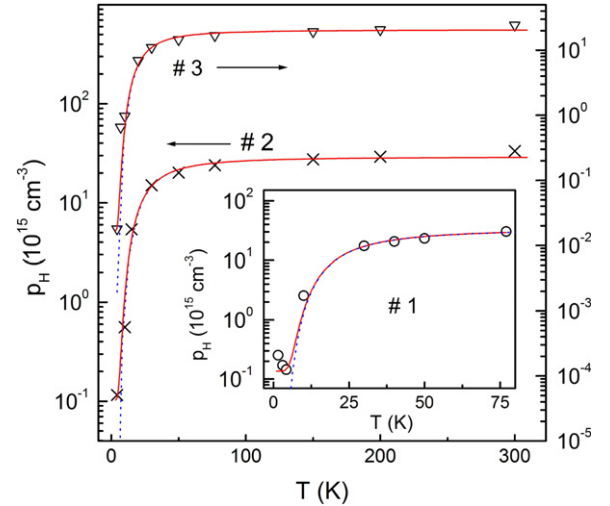


Figure 5. Temperature dependences of p_H in the investigated samples. The lines are calculated as described in the text.

increases with decreasing temperature. The dependence of $R_0(T)$ above ~ 50 K is weak, but it is considerably strengthened with lowering T , exhibiting a monotonous growth of R_0 down to 4.2 K. In sample 1, the Hall resistivity could be measured down to 1.5 K showing a decrease of R_0 when T is decreased between 4.2 and 1.5 K.

Treating the normal contribution to the Hall effect classically by restricting the analysis only to itinerant carriers, and taking the Hall factor equal to unity, the concentration of the holes can be written as $p_H = 1/(eR_0)$ shown versus temperature in figure 5. The behavior of $p_H(T)$ in the interval of extrinsic conductivity between ~ 4.2 and 200 K is entirely determined by the holes activated from acceptors to the VB with the concentration $p_V(T)$ and by the holes in the extended states of the AB, having the fraction α , with the concentration $\alpha p_A(T)$:

$$p_H(T) = p_V(T) + \alpha p_A(T), \quad (2)$$

where $p_A(T)$ is the total concentration of the holes in the AB, including those in the extended states and in the localized states. The latter make no contribution to the classical Hall effect, which restrict our analysis by the interval of $T \geq 4.2$ K, because at lower temperatures the hopping charge transfer over the localized states of the AB becomes important [7]. The upper limit of ~ 200 K guarantees the absence of the intrinsic contribution to $p_H(T)$, the latter being non-vanishing in CdSb already at 300 K [6]. Taking into account non-degeneracy of the holes in our samples [7], we can write for the terms in equation (2):

$$p_V(T) = N_V(T) \exp[-\xi/(kT)] \quad (3)$$

and

$$p_A(T) = 2N_A/\{1 + \exp[-(E_A - x)/(kT)]\}, \quad (4)$$

where $\xi = E_V - \eta$, $E_A = E_V - E_A^{(0)}$, η is the chemical potential, E_V and $E_A^{(0)}$ are the positions of the edge of the VB and of the maximum of the AB, respectively (the energy is measured toward the depth of the VB), $N_V(T) = 2(2mkT)^{3/2}/(4\pi^{3/2}\hbar^3)$ and $m = 0.2m_0$ is the mean effective mass of the holes

in CdSb (m_0 is the free electron mass) [6, 12]. In equation (3), we took into account the existence of the two equivalent maxima of the VB of CdSb [6] by introducing the multiplier 2 in the factor $N_V(T)$, and equation (4) corresponds to one unsplit by spin AB (neglecting the Hubbard correlations), where the spin degeneracy of the states of the AB is taken into account by introducing the multiplier 2 in the right-hand side of equation (4). Finally, the conservation of the holes satisfies the equation:

$$p_A(T) + p_V(T) = N_A(1 - K), \quad (5)$$

where $K = N_D/N_A$ is the degree of compensation and N_D is the concentration of compensating donors.

Excluding ξ from equation (4) with equation (3) and substituting equation (4) into equation (5), we obtain an equation containing a single unknown function $p_V(T)$, which can be solved numerically. Then $p_A(T)$ can be calculated with equation (5) and $p_H(T)$ can be evaluated with equation (2). The functions $p_H(T)$ are shown in figure 5 (solid lines). In calculations we use the values of E_A and N_A from [7] (see section 1), the values of $K = 5.5\%$, 13.4% and 17.7% for samples 1, 2 and 3, respectively, are obtained by fitting the high-temperature parts of $p_H(T)$ and the values of $\alpha = 4 \times 10^{-3}$, 3.5×10^{-3} and 0.8×10^{-3} for samples 1, 2 and 3, respectively, by fitting $p_H(T)$ on the low-temperature interval. Good agreement can be seen between the calculated and the experimental data of $p_H(T)$ for all our samples between 4.2 and 200 K, corresponding to the interval of applicability of the model given by equations (2)–(5) as discussed above. In addition, the calculations with $\alpha = 0$ (i.e. assuming $p_H = p_V$) are shown with the dotted lines in figure 5, which deviate from those with $\alpha \neq 0$ only below ~ 10 K. The values of $\alpha \ll 1$ demonstrate the existence of only a quite narrow interval of the extended states in the AB and negligible role of the itinerant holes of the AB in the formation of the normal contribution to the Hall effect, excluding the lowest temperatures as has been supposed above.

As follows from the top panel of figure 4, the temperature dependence of the anomalous contribution to ρ_H is similar to that of $R_0(T)$ on the bottom panel of figure 4, comprising the weak variation of $\rho_A(T)$ above ~ 50 K and a very strong increase with decreasing T from ~ 50 K to 4.2 K. In addition, the low-temperature drop of ρ_A in 1 resembles that of $R_0(T)$ in the region of hopping conductivity below 4.2 K. One can also see large scattering of the data of $\rho_A(T)$, exceeding considerably the error of determination of this parameter from the high-field linear approximation of $\rho_H(B)$ in figures 1–3. The normalization of ρ_A by M_s in figure 6 leads to closing in the values of ρ_A/M_s for different samples, but it cannot diminish the scattering of the data taking place even for one and the same sample, because M_s does not depend on T by definition (the data of M_s are taken from [2]—see section 1).

Because various microscopic models of AHE predict the power-law scaling of ρ_A with respect to ρ , i.e. the relations like $\rho_A \sim \rho^n$, where n is a constant (see below), we should compare the dependences of $\rho_A(T)$ and $\rho(T)$ rather than those of $\rho_A(T)$ and $R_0(T)$, despite the more similar behavior in the last pair. Indeed, the dependence of $\rho_A(T)$ resembles ρ

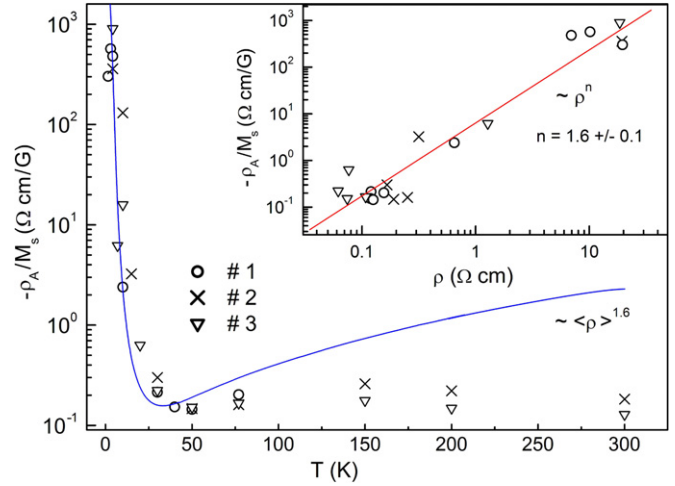


Figure 6. The dependence of ρ_A/M_s in the investigated samples. The line is the low-temperature fit to the experimental data with the function $\langle \rho(T) \rangle^{1.6}$. Inset: ρ_A/M_s versus ρ in the double-logarithm scale with the line as a linear fit.

(T) only below ~ 50 – 77 K (see the inset to the top panel of figure 4, where the data of ρ are taken from [7]), i.e., on the interval where the temperature dependence of the resistivity is determined presumably by the concentration of the itinerant holes, and deviates at higher T where $\rho(T)$ is governed by the temperature dependence of the hole mobility. On the other hand, this suggests that $\rho_A(T)$ in our material is mainly determined by the concentration of the charge carriers and is less sensitive to the scattering mechanisms. Anytime, below ~ 50 – 77 K all the three parameters $\rho_A(T)$, $R_0(T)$ and $\rho(T)$ behave in a similar way, exhibiting a strong upturn with lowering T , therefore we plotted ρ_A/M_s versus ρ at $T \leq 77$ K, where $\rho(T)$ for each sample is taken from the inset to the upper panel of figure 4 in a double-logarithm scale to test the possibility of the power-law scaling above. The linear approximation of the data in figure 6 yields $n = 1.6 \pm 0.1$ within four decades of ρ_A/M_s and more than two decades of ρ . Also from the main part of figure 6, it follows that ρ_A/M_s decays between ~ 1.5 and 77 K according to the power law $\langle \rho(T) \rangle^{1.6}$, where $\langle \rho(T) \rangle$ is the mean resistivity obtained by averaging the plots in the inset to the upper panel of figure 4.

For FM materials the values of $n = 1$ and 2 have been predicted by the microscopic models taking into account two different mechanisms of AHE, namely the skew scattering [20] and the side jump [21], respectively, both induced by the spin–orbit coupling. In a theory of multiband FM metals with dilute impurities [22], the power-law dependence $\sigma_A \sim \sigma^n$ of the anomalous Hall conductivity, σ_A , on the conductivity σ is shown to have an extrinsic-to-intrinsic crossover with n depending on the value of σ . Namely, the extrinsic skew scattering mechanism prevails in a clean limit with high conductivity yielding $n = 1$, whereas the intrinsic contribution becomes dominant in a dirty limit with low σ leading to $n = 1.6$. On the other hand, for diluted magnetic semiconductors with intrinsic FM behavior the intrinsic Berry phase theory of the AHE predicts the relation of $\rho_A \sim \rho^n$ with $n = 2$, too [23].

Experimentally, in FM metals the values of $n = 1$ and 2 in the law $\rho_A \sim \rho^n$ were already observed for a long time [14, 15].

Among the more recent results obtained in other materials, one can mention the value of $n = 1.9$ between the two limits of $n = 1$ and 2 in the models above, found for heterostructures (In, Mn) As/(Ga, Al) Sb [10], and $n \approx 0.6$ outside these limits, as determined in granulated films of Fe/SiO₂ [24]. On the other hand, neither the laws $R_s \sim \rho^n$ with $n = 1$ or 2 , nor their combination $R_s = (a\rho + b\rho^2)$ were found to interpret the AHE in the colossal magnetoresistive oxides La_{1-x}Ca_xCoO₃ [18] and La_{2-2x}Sr_{1+2x}Mn₂O₇ [19].

The experimental data above demonstrate non-universality of n in the power-law scaling $\rho_A \sim \rho^n$, which is in line with the absence of a universal mechanism of AHE in various FM systems. However, the analysis of the literature data of AHE in 28 different compounds, belonging to five different types of FM materials, suggests a broad universality class of the value of $n \approx 1.6$ in another law, $\sigma_A \sim \sigma^n$, being valid within over than five decades of σ irrespective of metallic or activated (and even hopping) conduction [17]. This value of n coincides with one of the predictions of the model [22], which, however, assumes only the metallic conductivity. Therefore, the universality of $n \approx 1.6$ in the law $\sigma_A \sim \sigma^n$ seems to have more general meaning.

Hence, the same value of $n = 1.6 \pm 0.1$ obtained by the analysis of our resistivity data (figure 6) may reflect the general universality established in [17]. On the other hand, as can be seen from figure 4, the values of ρ , ρ_A and ρ_N are comparable below ~ 77 K, where the power-law scaling is observed (the inset to figure 6). This hinders obtaining σ_A from our data unambiguously, which suggests a strong domination of the anomalous contribution to the Hall effect, and obtaining the exponent in the law $\sigma_A \sim \sigma^n$, being a subject of analysis in [17]. In addition, as has been mentioned above, our material is not ferromagnetic. The point is that the array of Ni_{1-x}Sb_x nanoclusters possesses features of an FM system only partially because, due to large-size distribution (see section 1), the unblocked clusters exist even below the blocking temperature T_b [2]. At this point, the large scattering of the data of ρ_A (figures 4 and 6) may reflect the existence of such unblocked clusters. Another feature of AHE in our material is also attributable to its poor similarity to FM systems, namely a linear dependence of $\rho_H(B)$ occurs above ~ 10 T (figures 1–3), whereas the magnetization has already saturated above ~ 2 T [2], which implies that $\rho_A(B)$ does not match the behavior of $M(B)$ in detail. Therefore, strictly speaking, neither of the models developed for FM systems above can be applied to our case directly, which does not permit us to make a final inference on the mechanism of AHE in our material.

3. Conclusions

We have investigated the Hall effect in single crystals of p-CdSb:Ni between 1.5 and 300 K in pulsed-magnetic fields up to 25 T. The dependence of the Hall resistivity $\rho_H(B)$ exhibits both the normal, $\rho_N(B) = R_0B$, and the anomalous, ρ_A , contributions, which follows from the nonlinearity of $\rho_H(T)$ being strongest at low temperatures but still existing

even at 300 K. The temperature dependence of the normal Hall coefficient R_0 is determined by activation of holes from acceptors into the valence band with a small contribution of the itinerant holes from the acceptor band at lowest T . The dependence of ρ_A on T is weak at high temperatures and is very strong below ~ 50 K, the latter resembling that of the resistivity, ρ . Below ~ 77 K the power-law scaling $\rho_A \sim \rho^n$ with $n = 1.6 \pm 0.1$ is observed within four decades of ρ_A and more than two decades of ρ . The anomalous Hall effect is attributable to magnetic Ni_{1-x}Sb_x nanoclusters, whose presence in p-CdSb:Ni has been established in investigations of the magnetic properties [2].

References

- [1] Žutić I, Fabian J and Das Sarma S 2004 *Rev. Mod. Phys.* **76** 323
- [2] Laiho R, Lashkul A V, Lisunov K G, Lähderanta E, Ojala I and Zakhvalinskii V S 2006 *Semicond. Sci. Technol.* **21** 228
- [3] Marenkin S F, Saidullaeva M, Sanygin V P and Kovaleva I S 1982 *Izv. Akad. Nauk SSSR, Neorg. Mater.* **18** 1759
- [4] Hoselitz K 1952 *Ferromagnetic Properties of Metals and Alloys* (Oxford: Clarendon)
- [5] Kneller E 1962 *Ferromagnetismus* (Berlin: Springer)
- [6] Arushanov E K 1986 *Prog. Cryst. Growth Charact.* **13** 1
- [7] Laiho R, Lashkul A V, Lisunov K G, Lähderanta E, Shakhov M A and Zakhvalinskii V S 2008 Hopping conductivity of Ni-doped p-CdSb *J. Phys.: Condens. Matter* **20** 295204
- [8] Laiho R, Lashkul A V, Lisunov K G, Lähderanta E, Shakhov M A and Zakhvalinskii V S 2008 Hopping conductivity of Ni-doped p-CdSb in strong magnetic fields *J. Phys. Chem. Solids* at press
- [9] Shinde S R, Ogale S B, Higgins J S, Zheng H, Millis A J, Kulkarni V N, Ramesh R, Greene R L and Venkatesan T 2004 *Phys. Rev. Lett.* **92** 166601
- [10] Oiwa A, Endo S, Katsumoto S, Iye Y, Ohno H and Munekata H 1999 *Phys. Rev. B* **59** 5826
- [11] Lengsfeld P, Brehme S, Ehlers G, Lange H, Stusser N, Tomm Y and Fuhs W 1998 *Phys. Rev. B* **58** 154
- [12] Laiho R, Lashkul A V, Lisunov K G, Lähderanta E, Safonchik M O and Shakhov M A 2004 *Semicond. Sci. Technol.* **19** 602
- [13] Laiho R, Lashkul A V, Lisunov K G, Lähderanta E, Safonchik M O and Shakhov M A 2006 *Semicond. Sci. Technol.* **21** 918
- [14] Berger L and Bergmann G 1980 *The Hall Effect and its Applications* (New York: Plenum)
- [15] Vonsovskii S V 1971 *Magnetism* (Moscow: Nauka)
- [16] Yuldashev Sh U, Jeon H C, Im H S, Kang T W, Lee S H and Furdyna J K 2004 *Phys. Rev. B* **70** 193203
- [17] Fukumura T, Toyosaki H, Ueno K, Nakano M, Yamasaki T and Kawasaki M 2007 *Japan. J. Appl. Phys.* **46** L 642
- [18] Samoilov A V, Beach G, Fu C C, Yeh N-C and Vasquez R P 1998 *Phys. Rev. B* **57** 032
- [19] Hirobe Y, Ashikawa Y, Kawasaki R, Noda K, Akahoshi D and Kuwahara H 2006 *Solid State Commun.* **137** 191
- [20] Smith J 1958 *Physica* **24** 39 (Amsterdam)
- [21] Berger L 1970 *Phys. Rev. B* **2** 4559
- [22] Onoda S, Sugimoto N and Nagaoka N 2006 *Phys. Rev. Lett.* **97** 126602
- [23] Jungwirth T, Niu Q and MacDonald A H 2002 *Phys. Rev. Lett.* **88** 207208
- [24] Aronson B A, Kovalev D Yu, Lagarkov A N, Meilikhov E Z, Rylkov V V, Sedova M A, Negre N, Goiran M and Leotin J 1999 *JETP Lett.* **70** 90